On Space-Time Rake Receiver Structures for WCDMA

Christopher Brunner,[1,2] *Martin Haardt,*[1] *and Josef A. Nossek*[2]

1. Siemens AG, ICN CA CTO 7
Hofmannstr. 51, D-81359 Munich, Germany
Phone / Fax: +49 (89) 722-29480 / -44958
E-Mail: Martin.Haardt@icn.siemens.de

2. Institute for Circuit Theory and Signal Processing
Munich Univ. of Technology, D-80290 Munich, Germany
Phone / Fax: +49 (89) 289-28511 / -28504
E-Mail: Christopher.Brunner@ei.tum.de

Abstract

Adaptive space-time rake receivers use diversity combining and multi-user interference suppression to obtain a considerable increase in performance in DS-CDMA systems such as Wideband CDMA (WCDMA). In this paper, we compare the structure and performance of different space-time rake receivers for WCDMA. After a review of the decoupled space-time rake and the joint space-time rake, we present a new joint space-time rake with spatial and temporal compression matrices. Here, the spatial compression matrix is calculated from spatial covariance matrices that can be averaged over several time slots, since the change of the spatial characteristics is much slower than the fast fading. It has more degrees of freedom than the decoupled space-time rake, but less than the joint space-time rake. Finally, Monte-Carlo simulations demonstrate the performance of several space-time rake structures for different scenarios. It turns out that if good spatio-temporal channel estimates are available (e.g., in case of a small Doppler), more degrees of freedom can be exploited by the space-time rake receiver structure.

1. Introduction

Adaptive antennas exploit the inherent spatial diversity of the mobile radio channel, provide an antenna gain, and enable spatial interference suppression and are, therefore, seen as an important technology to meet the high spectral efficiency and quality requirements of third generation mobile radio systems. The proposed concepts for the third generation [6] allow an easy and flexible implementation of new and more sophisticated services. The 3rd Generation Partnership Project (3GPP) has selected the TD-CDMA concept as the radio access scheme for third-generation (3G) time-division duplex (TDD) systems and the WCDMA concept for 3G frequency-division duplex (FDD) systems. This solution had previously been contributed to the International Telecommunication Union by ETSI SMG - as the European proposal for IMT-2000 transmission technology.

In WCDMA, there are connection-dedicated control channels. The known pilot symbols that are transmitted on these *control channels* can be exploited for channel estimation to obtain the weights for the different space-time rake receiver structures [2]. In case of the joint space-time rake and the compressed space-time rake, it is sufficient to estimate the instantaneous signal space-time covariance matrix which has rank one. Thus, we solve a set of equations instead of a generalized eigenvalue problem [2], which reduces the computational complexity considerably. Then the estimated spatial, temporal, or space-time weight vectors are applied to the corresponding *data channel* to obtain estimates of the transmitted data symbols, cf. Figures 2, 3, and 4.

Note that the concept of the compressed space-time rake is related to the reduced dimension space-time rake introduced in [3]. However, instead of using a parameter estimation scheme to obtain the channel parameters such as delays and directions of arrival, we use a simple rake searcher to obtain the delays. The directions of arrival are not estimated explicitly. Instead, the spatial compression vectors are estimated from spatial covariance matrices, which can take into account angular spread and, if we do not average over many slots, spatial diversity.

2. WCDMA Uplink Signal Model

WCDMA has two types of dedicated physical channels on the uplink as well as the downlink, the dedicated physical control channel (DPCCH) and the dedicated physical data channel (DPDCH). In case of low and medium data rates, one connection consists of one DPCCH and one DPDCH which are code and IQ multiplexed in the uplink [6]. The DPDCH baseband signal of the user of interest may be expressed as

$$s_{\mathrm{D}}(t) = \sum_{\ell=-\infty}^{\infty} b_{\mathrm{D}}^{(\ell)}\, z_{\mathrm{D}}(t-\ell T_{\mathrm{D}}), \quad z_{\mathrm{D}}(t) = \sum_{j=1}^{Q_{\mathrm{D}}} d_{\mathrm{D}}^{(j)}\, p(t-jT_c).$$

0-7803-5700-0/99/$10.00©1999 IEEE

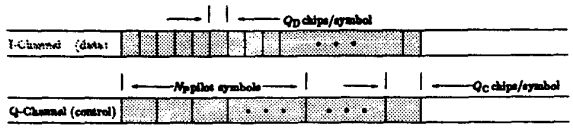

Figure 1. Uplink slot structure of WCDMA: A combination of code and IQ multiplexing is used. Moreover, N_P pilot symbols are transmitted at the beginning of each DPCCH slot.

The used chip rate is $1/T_c = 4.096$ Mchips/s. Moreover, the spreading sequence of the DPDCH, $z_D(t)$, is of length $T_D = Q_D T_c$ and is composed of Q_D chips $d_D^{(j)} \in \{-1, 1\}$, $1 \leq j \leq Q_D$. The symbols, $b_D^{(\ell)} \in \{-1, 1\}$, are BPSK modulated. WCDMA uses a chip waveform, $p(t) \in \mathbb{R}$, characterized by a square-root raised cosine spectrum with a rolloff factor of $\alpha = 0.22$. In the same way, the DPCCH baseband signal of the user of interest is given by

$$s_C(t) = \sum_{\ell=-\infty}^{\infty} b_C^{(\ell)} z_C(t-\ell T_C), \quad z_C(t) = \sum_{j=1}^{Q_C} d_C^{(j)} p(t-jT_c),$$

where the spreading sequence of the DPCCH, $z_C(t)$, is of length $T_C = Q_C T_c$.

Note that DPDCH and DPCCH may use different spreading codes. Then they are mapped to the I and Q branches according to [6]

$$s(t) = \beta \cdot s_D(t) + \mathrm{j} \cdot s_C(t), \tag{1}$$

where β denotes the power of the DPDCH in relation to the DPCCH. Next, the complex I+jQ signal is either scrambled by a complex long code of 40960 chips in case of single user detection [6] (or by a complex short code of 256 chips in case of multiuser detection). For simplicity, we do not include scrambling in our notation.

3. Space-Time Rake Structures

3.1. Channel Model

In the sequel, adaptive antennas are assumed at base stations only. Moreover, we assume that the narrowband assumption holds. Then each wavefront arriving at different antenna elements can be characterized by a phase shift. Hence, the baseband representation of the $M \times 1$ array snapshot vector $\boldsymbol{x}(t)$ containing the outputs of each of the M antenna elements after the channel filter at time t is modeled as

$$\begin{aligned} \boldsymbol{x}(t) &= \sum_{i=1}^{L_1} \xi_i^{(1)} \boldsymbol{a}^{(1)}(\mu_i) s^{(1)}(t - \tau_i^{(1)}) * p(t) \\ &+ \sum_{k=2}^{K} \sum_{i=1}^{L_k} \xi_i^{(k)} \boldsymbol{a}^{(k)}(\mu_i) s^{(k)}(t - \tau_i^{(k)}) * p(t) + \boldsymbol{n}(t), \end{aligned} \tag{2}$$

where $\boldsymbol{a}^{(k)}(\mu_i)$, $\tau_i^{(k)}$, and $\xi_i^{(k)}$ denote the steering vector, the delay, and the complex amplitude of the i-th wavefront of the k-th user, respectively. Furthermore, L_k is the number of impinging wavefronts of the kth user, and the convolution operator is denoted by $*$. In this paper, user 1 is the user of interest. In the sequel, we assume that the different receivers are synchronized to the beginning of a slot. Moreover, the (over)sampled output of each antenna element is passed through a correlator of N_P pilot symbols to estimate the spatial, temporal, or space-time weight vectors.

3.2. Decoupled Space-Time Rake

The beamformer rake receiver originally proposed in [4, 5] can be interpreted as a decoupled space-time rake receiver, i.e., there is a spatial beamformer for each of the N_f rake fingers, followed by a temporal rake combiner. Its application to WCDMA is depicted in Fig. 2.

To calculate the spatial weights, a rake searcher determines the positions of the N_f rake fingers *after* the correlation with the pilot sequence. At the position of each rake finger, we estimate the spatial covariance matrix of the signal of interest, which is denoted as $\hat{\boldsymbol{R}}_S^{(n)}$, $1 \leq n \leq N_f$. The spatial covariance matrix of the signal-plus-interference-plus-noise $\boldsymbol{R}_{SIN}$ is estimated *before* the correlator by averaging over several spatial snapshots.

According to [5], the interference-plus-noise (IN) covariance matrix estimate for the n-th finger is calculated as

$$\hat{\boldsymbol{R}}_{IN}^{(n)} = \frac{Q_C}{Q_C - 1} \left(\hat{\boldsymbol{R}}_{SIN} - \frac{1}{Q_C} \hat{\boldsymbol{R}}_S^{(n)} \right). \tag{3}$$

Then the spatial weight vector at the n-th finger $\boldsymbol{w}_n$, $1 \leq n \leq N_f$, is given by the eigenvector corresponding to the largest generalized eigenvalue of the generalized eigenvalue problem[1]

$$\hat{\boldsymbol{R}}_S^{(n)} \boldsymbol{w}_n = \lambda \hat{\boldsymbol{R}}_{IN}^{(n)} \boldsymbol{w}_n. \tag{4}$$

After the spatial filters, another channel estimate (correlation with the known pilot symbols) is required to find the weights of the subsequent temporal rake combiner (temporal matched filter). This is also illustrated in Fig. 2. It can be seen how the spatial and temporal weight vectors are applied to the data channel.

In contrast to the temporal weight vectors which should be updated in every time slot to track the fast fading, the spatial covariance matrix estimates $\hat{\boldsymbol{R}}_S^{(n)}$ and $\hat{\boldsymbol{R}}_{SIN}$ (that are used to calculate the spatial weight vectors) can be averaged over several slots to improve the channel estimation accuracy, since the change of the spatial characteristics is much slower than the fast fading.

[1] If the processing gain of the control channel (that incorporates the known pilot symbols) is very high, we can replace (4) by $\hat{\boldsymbol{R}}_S^{(n)} \boldsymbol{w}_n = \lambda \hat{\boldsymbol{R}}_{SIN} \boldsymbol{w}_n$.

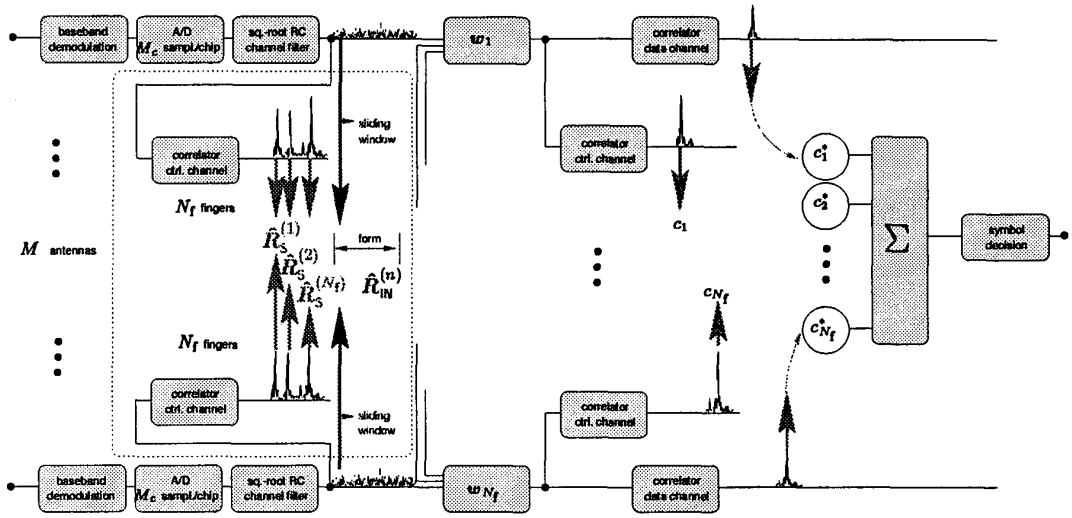

Figure 2. Structure of the decoupled space-time rake (beamformer rake).

3.3. Joint Space-Time Rake

Next, we present a rake receiver that performs *joint* space-time processing. This joint space-time rake is depicted in Fig. 3.

Let us assume that the rows of the data matrices $\mathcal{X} \in \mathbb{C}^{M\times N}$ and $\mathcal{Y} \in \mathbb{C}^{M\times N}$ contain the spatial snapshots $\boldsymbol{x}(t)$ and $\boldsymbol{y}(t)$ sampled at M_c times the chip rate $1/T_c$ *before* and *after* the correlator, respectively. Then a temporal selection matrix

$$\boldsymbol{J}^{(i)} = \begin{bmatrix} \boldsymbol{0}_{(i-1)\times N_w} \\ \boldsymbol{I}_{N_w\times N_w} \\ \boldsymbol{0}_{(N-i-N_w+1)\times N_w} \end{bmatrix}$$

is applied to the correlator output $\mathcal{Y}$ such that $\mathcal{Y}\boldsymbol{J}^{(1)} \in \mathbb{C}^{M\times N_w}$ contains all multipath components. This is illustrated in Fig. 3. The maximum channel delay spread in samples is denoted by $N_w = M_c\frac{\tau_{\max}}{T_c}$, where M_c is the oversampling factor and $\tau_{\max}$ is the maximum delay spread. The temporal selection matrix acts as a sliding window for an increasing index i. Its outputs $\mathcal{X}\boldsymbol{J}^{(i)}$ are averaged to estimate the space-time SIN covariance matrix *before* the correlator[2]. To this end, we define the space-time snapshots *before* and *after* the correlator as $\boldsymbol{x}_{\text{ST}}^{(i)} = \text{vec}\{\mathcal{X}\boldsymbol{J}^{(i)}\}$ and $\boldsymbol{y}_{\text{ST}} = \text{vec}\{\mathcal{Y}\boldsymbol{J}^{(1)}\}$, respectively. The vec-operator maps an $m \times n$ matrix into an mn-dimensional column vector by stacking the columns of the matrix. Assuming that the channel stays approximately constant for at least one slot, the space-time covariance matrix of the signal of interest

$$\hat{\boldsymbol{R}}_{\text{S}}^{(\text{ST})} = \boldsymbol{y}_{\text{ST}} \cdot \boldsymbol{y}_{\text{ST}}^H \tag{5}$$

is estimated by using only one space-time snapshot that contains the multipaths of the user of interest, cf. Fig. 3. Note that $\hat{\boldsymbol{R}}_{\text{S}}^{(\text{ST})}$ has rank one.

The space-time signal-plus-interference-plus-noise (SIN) covariance matrix is estimated *before* the correlator as

$$\hat{\boldsymbol{R}}_{\text{SIN}}^{(\text{ST})} = \text{mean}\left\{\boldsymbol{x}_{\text{ST}}^{(i)} \cdot \boldsymbol{x}_{\text{ST}}^{(i)H}\right\}. \tag{6}$$

Then an estimate of the space-time IN covariance matrix $\hat{\boldsymbol{R}}_{\text{IN}}^{(\text{ST})}$ is calculated according to

$$\hat{\boldsymbol{R}}_{\text{IN}}^{(\text{ST})} = \frac{Q_{\text{C}}}{Q_{\text{C}}-1}\left(\hat{\boldsymbol{R}}_{\text{SIN}}^{(\text{ST})} - \frac{1}{Q_{\text{C}}}\hat{\boldsymbol{R}}_{\text{S}}^{(\text{ST})}\right). \tag{7}$$

The joint space-time weight vector $\boldsymbol{w}$ is given by the eigenvector corresponding to the largest generalized eigenvalue of the generalized eigenvalue problem[3]

$$\hat{\boldsymbol{R}}_{\text{S}}^{(\text{ST})}\boldsymbol{w} = \lambda\hat{\boldsymbol{R}}_{\text{IN}}^{(\text{ST})}\boldsymbol{w}. \tag{8}$$

By taking into account (5), we can divide both sides of (8), by the scalar $\boldsymbol{y}_{\text{ST}}^H\boldsymbol{w}$, yielding

$$\boldsymbol{y}_{\text{ST}} = \hat{\boldsymbol{R}}_{\text{IN}}^{(\text{ST})}\boldsymbol{w}', \tag{9}$$

where $\boldsymbol{w}'$ is a scaled version of $\boldsymbol{w}$. Hence, the joint space-time weight vector can be found by solving the linear system of equations (9). This system of equations could be solved directly, e.g., via a Cholesky decomposition of $\hat{\boldsymbol{R}}_{\text{IN}}^{(\text{ST})}$ or iteratively, e.g., via a Gauss-Seidel iteration that uses the space-time weight vector from the previous slot as an initial value, cf. [2]. It is applied to the data channel as illustrated in Fig. 3.

[2] In the sequel, we do not average over fast fading. Therefore, i is limited to the spatial snapshots with the same spatial and temporal channel properties.

[3] Again, if the processing gain of the control channel (that incorporates the known pilot symbols) is very high, we can replace (8) by $\hat{\boldsymbol{R}}_{\text{S}}^{(\text{ST})}\boldsymbol{w} = \lambda\hat{\boldsymbol{R}}_{\text{SIN}}^{(\text{ST})}\boldsymbol{w}$.

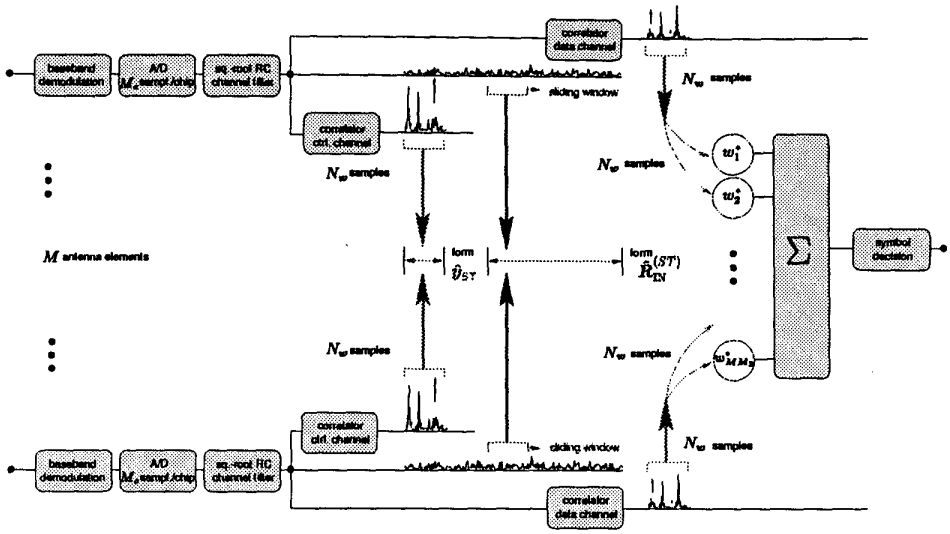

Figure 3. Structure of the joint space-time rake.

3.4. Compressed Space-Time Rake

Finally, we define spatial and temporal compression matrices to reduce the computational complexity of the joint space-time rake especially in case of long delay spreads. Moreover, its performance is improved, since the spatio-temporal structure of the mobile radio channel is exploited even further. To this end, we construct a spatial compression matrix from the spatial beamforming vectors calculated in Subsection 3.2 according to

$$C_S = [\ w_1 \quad w_2 \quad \cdots \quad w_{N_f}\ ] \in \mathbb{C}^{M \times N_f}. \tag{10}$$

Likewise, we can construct a temporal compression matrix $C_T \in \mathbb{R}^{N_w \times N_f}$. All entries of n-th column of C_T are "0"s, except for a single "1" at the position of the n-th rake finger. This position can be determined by a conventional rake searcher. Then the compressed space-time vectors *before* and *after* the correlator are defined as

$$x_c^{(i)} = \mathrm{vec}\left\{C_S^H \mathcal{X} J^{(i)} C_T\right\} \tag{11}$$

and

$$y_c = \mathrm{vec}\left\{C_S^H \mathcal{Y} J^{(1)} C_T\right\}, \tag{12}$$

respectively[4]. Hence, we get

$$\hat{R}_S^{(C)} = y_c \cdot y_c^H \tag{13}$$

and

$$\hat{R}_{SIN}^{(C)} = \mathrm{mean}\left\{x_c^{(i)} \cdot x_c^{(i)H}\right\}. \tag{14}$$

Then the compressed space-time IN covariance matrix $\hat{R}_{IN}^{(C)}$ is calculated as before, cf. (7). Finally, the compressed space-time weight vector w_c' can be found by solving

$$y_c = \hat{R}_{IN}^{(C)} w_c'. \tag{15}$$

The structure of the resulting compressed space-time rake is depicted in Fig. 4.

4. Simulations

The mobile radio channel can be characterized by its Doppler, by its spatial diversity, and by its angular and delay spread.

- In case of a small Doppler, the channel estimate is improved by averaging this estimate over more than one slot.
- A spatially structured channel (small spatial diversity orders at the corresponding fingers) enables spatial preprocessing to improve the channel estimate[5].
- Scenarios in which users have a delay spread and differing directions of arrival at different taps are best served by joint space-time or space-frequency processing, given that a good channel estimate is available.

In general, the less the channel is known, i.e., the worse the channel estimate is, the fewer degrees of freedom should be available for the weight vector. For instance, the spatial and temporal weight vectors of the decoupled space-time rake (averaging the spatial covariance matrices) have the least, the joint space-time weight vector of the joint space-time

[4]Note that the diagonal elements of the matrix $C_S^H \mathcal{Y} J^{(1)} C_T \in \mathbb{C}^{N_f \times N_f}$ correspond to the temporal weights $c_1, \ldots, c_{N_f}$ used by the decoupled space-time rake, cf. Fig. 2.

[5]By varying the distance of the antenna elements, a tradeoff between spatial correlation (which yields an improved channel estimate if the spatial covariance matrices are averaged over many time slots) and spatial diversity can be achieved.

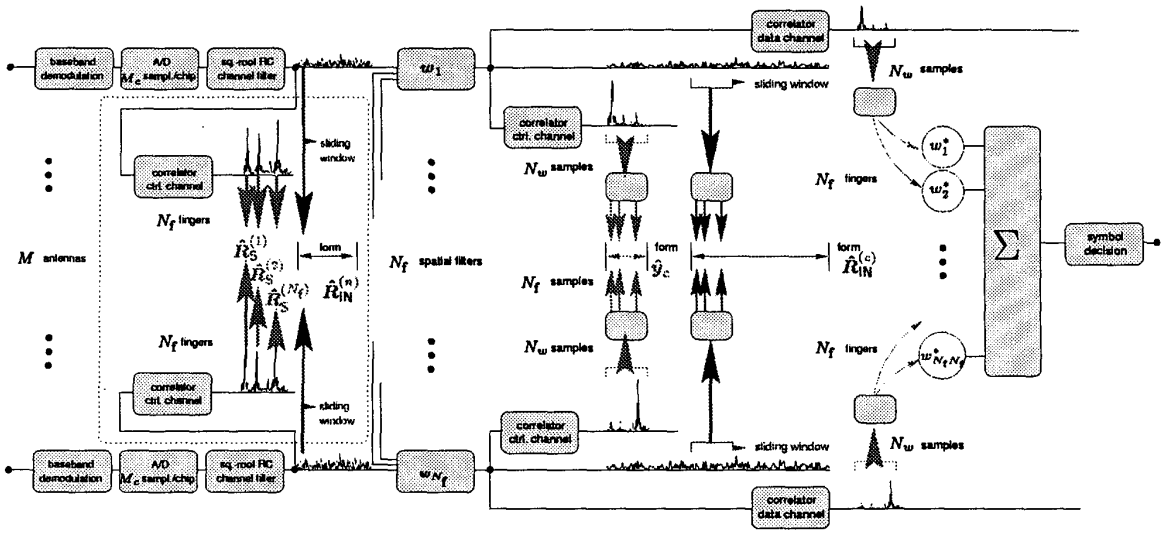

Figure 4. Structure of the joint space-time rake with spatial and temporal compression matrices (compressed space-time rake).

rake has the most degrees of freedom (N_f versus MN_w). The simulation results are based on a rural and a micro environment [1]. The rural scenario is characterized by a small delay spread, a large Doppler, and a spatially structured channel. The micro scenario, on the other hand, is characterized by a larger delay spread, a small Doppler, and a spatially unstructured channel.

In the simulations, we assume 14 high data-rate interferers and 70 speech interferers, which have a data channel spreading factor Q_D of 8 and 128, respectively. To compensate for the correlation gains, the high data-rate interferers are received at the base station with 16 times more power than the speech interferers[6].

The upper left plot of Fig. 5 describes the performance of the rake receiver structures (joint space-frequency rake [2], joint ST rake, decoupled ST rake with $\lambda = 0$, compressed ST rake, decoupled ST rake with $\lambda = 0.995$) for the rural scenario, where λ denotes the forgetting factor which is applied when estimating the spatial covariance matrices $\boldsymbol{R}_S^{(n)}$. The channel estimate is based on only one slot, the service of the user of interest is speech, the multipath spread is fixed at $N_w = 4$ samples, and $N_f = 2$ rake fingers per antenna hold. The structures which exploit the spatial structure of the channel perform best.[7]

[6]We have assumed perfect power control. To reduce simulation time, the weak interferers are modeled as spatially and temporally white noise which is passed through a channel filter before it is added to the channel.

[7]Due to a poor channel estimate, there are too many degrees of freedom for the joint space-time and joint space-frequency rake.

The remaining plots of Fig. 5 are based on the micro scenario, where $N_w = 13$ and $N_f = 3$ hold. In the upper right plot, the performance is plotted for a speech user of interest where the channel estimate is based on one slot, in the lower left plot, the channel estimate is based on the six previous slots, and in the lower right plot, again, the channel estimate is based on the six previous slots, however, assuming a high data-rate user of interest which is received with more power. Therefore, the channel estimate is best in the last case. Accordingly, the structures with the most degrees of freedom perform worst in the upper right plot and best in the lower right plot and vice versa.

Limits on hardware complexity necessitate a small number of rake fingers per antenna, N_f, to limit the number of correlations required for channel estimation and data detection. Typically, N_f is smaller than 5. Then the computational complexity required to obtain the weight vector is relatively small compared to the correlations.

5. Conclusions

In this paper, we have compared the structure and performance of different space-time rake receivers for WCDMA, which has been chosen as the radio access scheme for the (direct spread) FDD mode of 3rd generation mobile radio systems. The compressed space-time rake has more degrees of freedom than the decoupled space-time rake, but less than the joint space-time rake or the joint space-frequency rake. If an excellent channel estimate is available (e.g., in case of a small Doppler), space-time rake receiver structures with large degrees of freedom perform best and vice versa.

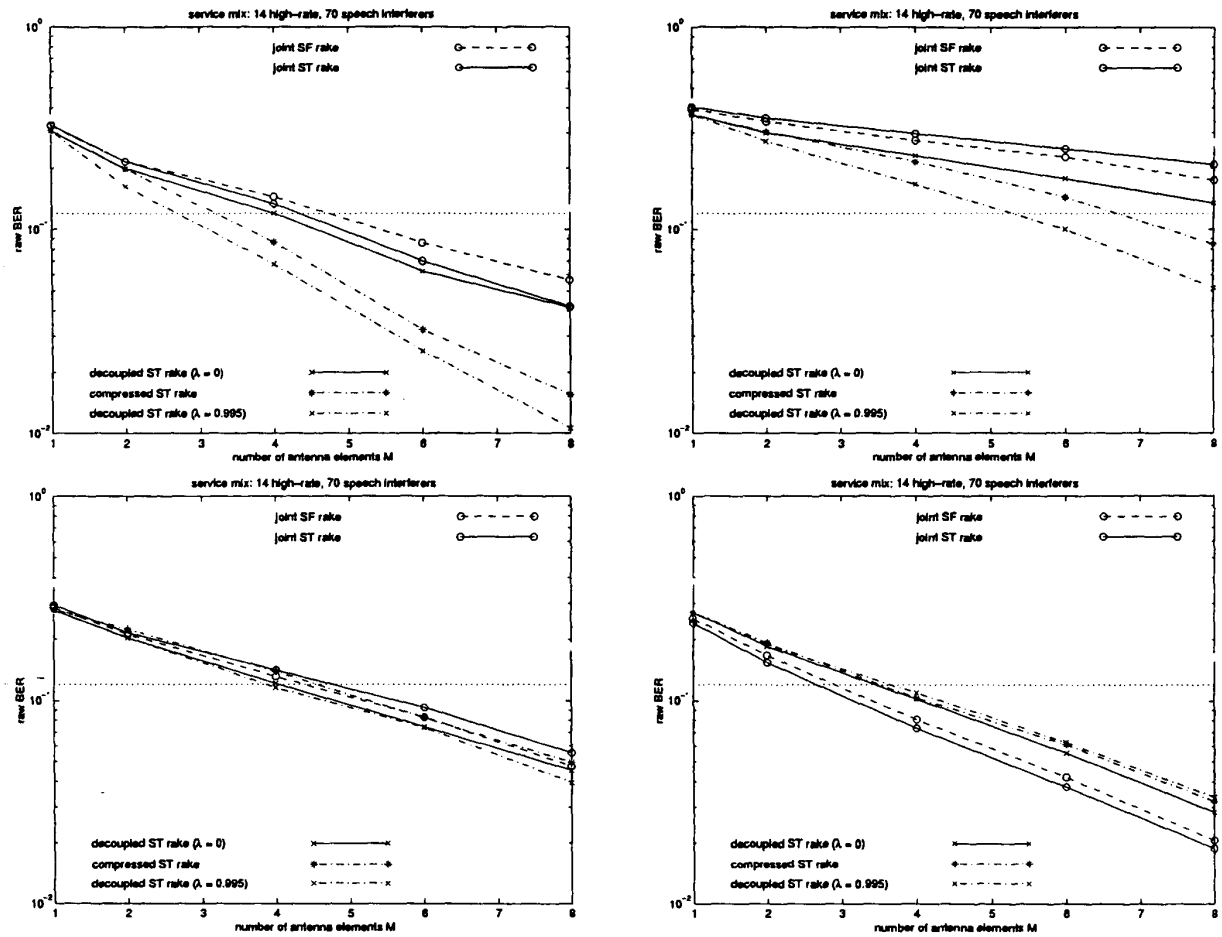

Figure 5. Our performance measure is the raw bit error ratio (BER). It is assumed that a raw BER smaller than 12 % is required to ensure a sufficient BER after decoding for uplink WCDMA (simulation parameters: uniform linear array: $\Delta = 0.5\lambda$, $M_c = 2$, $\beta = 2$, # of trials: 400 slots = 250 ms).

Acknowledgement

The authors would like to thank Alexander Seeger (Siemens AG, Munich) for many fruitful discussions.

References

[1] J. J. Blanz and P. Jung. A flexible configurable spatial model for mobile radio systems. *IEEE Trans. on Communications*, 46:367-371, Mar. 1998.

[2] C. Brunner, M. Haardt, and J. A. Nossek. Adaptive space-frequency rake receivers for WCDMA. In *Proc. IEEE Int. Conf. Acoust., Speech, Signal Processing (ICASSP '99)*, volume 4, pages 2383–2386, Phoenix, Arizona, Mar. 1999.

[3] Y. Chen and M. D. Zoltowski. Joint angle and delay estimation for DS-CDMA with applications to reduced dimension space-time rake receivers. In *Proc. IEEE Int. Conf. Acoust., Speech, Signal Processing (ICASSP '99)*, volume 5, May 1999.

[4] B. Khalaj, A. Paulraj, and T. Kailath. Spatio-temporal channel estimation techniques for multiple access spread spectrum systems with antenna arrays. In *Proc. IEEE International Conference on Communications (ICC '95)*, pages 1520–1524, 1995.

[5] A. F. Naguib. *Adaptive Antennas for CDMA Wireless Networks*. Ph. D. dissertation, Stanford University, Palo Alto, CA, Aug. 1996.

[6] E. Nikula, A. Toskala, E. Dahlman, L. Girard, and A. Klein. FRAMES Multiple Access for UMTS and IMT-2000. *IEEE Pers. Comm. Mag.*, Apr. 1998.